Sulfide emissions in sewer networks: Empirical and numerical modelling

Lucie Carrera, Fanny Springer, Gislain Lipeme Kouyi, Pierre Buffière

Sulfide emissions in sewer networks: Empirical and numerical modelling

Lucie Carrera[1], Fanny Springer[1], Gislain Lipeme Kouyi[1] and Pierre Buffiere[1]

1 Université de Lyon, INSA-Lyon, Laboratory of Wastes Water Environment Pollutions, France

**lucie.carrera@insa-lyon.fr; fanny.springer@insa-lyon.fr; gislain.lipeme-kouyi@insa-lyon.fr; pierre.buffiere@insa-lyon.fr*

Abstract

The relation between concrete corrosion and hydrogen sulfide emission was identified more than a century ago. Sulfide is produced by sulfate reducing bacteria (SRB) under the form of dissolved H_2S that can be emitted into the atmosphere. The conditions that enhance its transfer, and the associated emission kinetics, are of obvious importance. This work aimed at measuring the H_2S mass transfer coefficient as a function of the hydraulic characteristics of the flow with the objective of estimating the H_2S emission in gravity pipes, and collecting data to establish models independent of the system geometry. For this goal, several scales were investigated: at lab-scale, 8 L batch reactor device, similar to a homogeneous liquid volume was experimented and, at real-scale, a 10 m long and 0.2 m diameter gravity pipe device with continuous water flow was set up. Experimentally, the following ranges of values were investigated: velocity flow [0 - 0.61 $m.s^{-1}$], Reynolds number [0 – 23,333], and Froude number [0 – 0.97]. The CFD modeling tools ICEM CFD™ and FLUENT ™ v.14 software were used to determine the hydrodynamic parameters at the liquid/gas interface with accuracy, so as to link the mass transfer coefficients to local hydrodynamic parameters.

The O_2 mass transfer coefficient ($m.h^{-1}$) in the closed reactor was experimentally expressed with the stirring rate (rps) as follows $K_{L,O_2} = 0.015 + 0.025\ N^{3.91}$. A $K_{L,H2S}$ / $K_{L,O2}$ ratio of 0.64± 0.24 was determined. With the numerical modeling results, this correlation was refined and expressed as a function of the local interface parameter ui ($m.h^{-1}$) $\boldsymbol{K_{L,O2} = 0.015 + 1.35 \times 10^{-12}\ u_i^{3.91}}$. In the real-scale pipe device, $K_{L,O2}$ exponentially increased with the mean velocity. The exponential evolution of the mass transfer coefficient with the velocity is consistent with the increasing level of turbulence. In this system, hydraulic description of the flow was examined. The hydraulic conditions in the liquid-gas boundary layer, the local velocity and the Reynolds number, were extracted from the modeling results. With the correlations previously established, the expected O_2 mass transfer coefficients were calculated and compared to the experimentally measured mass transfer coefficients.

Keywords

H_2S emission, correlation, gravity pipe, reaeration, local turbulence intensity, numerical simulation.

SYMBOL

a = specific interfacial area ($m^2.m^{-3}$)
a_x = correlation coefficient ($m.h^{-1}$)
b_x, c_x = correlation coefficients (-)
$C_{L,i}$ = concentration in liquid phase of component i ($mg.L^{-1}$)
$C_{S,i}$ = saturation concentration of component i ($mg.L^{-1}$)
d = stirrer diameter (m)
$D_{m,i}$ = diffusivity coefficient of component i ($m^2.s^{-1}$)
d_m = hydraulic mean depth (m)
d_h= hydraulic diameter (m)
Fr_1 = Froude number for agitation (-)
Fr_2 = Froude number for flow (-)
g = standard gravity ($m.s^{-2}$)
h= the vortex deformation (height $h=h_{max}-h_{min}$) (m)
k= turbulent kinetic energy ($m^2.s^{-2}$)
$k_{L,i}$ = mass transfer coefficient of component i in liquid phase ($m.h^{-1}$)
$K_{L,i}$ = overall mass-transfer coefficient of component i ($m.h^{-1}$)
N = stirring rate (s^{-1})
n= coefficient
Re_1 = Reynolds number for agitation (-)
Re_2 = Reynolds number for flow (-)
Re_i = interface Reynolds number (-)
R_h = hydraulic radius (m)
s = slope ($m.m^{-1}$)
S= wetted surface (m^2)
t = time (t)
u = flow velocity ($m.s^{-1}$)
u_i= weighted velocity at the interface ($m.h^{-1}$)
z= distance (m)

Greek symbols
ε= turbulent energy dissipation ($m^2.s^{-3}$)
μ_L = viscosity of water ($Pa.s^{-1}$)
ρ_L = density of the continuous phase ($kg.m^{-3}$)

INTRODUCTION

The relation between concrete corrosion and hydrogen sulfide emission was identified more than a century ago. Sulfide is produced by sulfate reducing bacteria (SRB) under the form of dissolved H_2S that can be emitted into the atmosphere. The conditions that enhance its transfer, and the associated emission kinetics, are of obvious importance. Accumulation of H_2S in the sewer atmosphere in gravity sewer systems is a detrimental phenomenon for several reasons. First, in the presence of oxygen, sulfide is oxidized in sulfuric acid, which is corrosive and causes the disintegration of cement materials. This phenomenon is a real economic loss for communities, because it requires an accelerated rehabilitation and pipe replacement frequency. Second, inhalation of H_2S, even at relatively low concentrations, is toxic to humans. Many deaths during routine maintenance in sewers were attributed to H_2S toxicity. The sulfide problem will be accentuated in the future because of the temperature rising and the need to spread the cities.

Consequently, understanding the fate of sulfide is thus a major challenge for a better management of sewer systems. If the mechanism of sulfide production is quite known, the emission into the atmosphere is less described and deserves more attention (Carrera *et al.*, 2015). Since H_2S is produced in anaerobic conditions, the sulfuric cycle is linked to the oxygenation. The oxygen concentration in wastewaters and the hydrogen sulfide emission both depend on liquid-gas transfer phenomena in sewers (USEPA, 1974). The study of the sulfide emission at lab-scale and in situ is complex due to the hazardous properties of this gas and the lack of sensitive on-line analytical procedures. Two main approaches are developed in the literature: i) empiric or theoretical connections between oxygen and hydrogen sulfide transfer coefficients; ii) empiric models linking the sulfide emission to flow parameters.

Besides the danger of manipulating H_2S, the measurement of the mass-transfer coefficient for this compound is more difficult than for oxygen, because the available measurement methodologies are: i) the methylene blue method, a sensitive off-line analytical procedure that restrains the sampling frequency and the data acquisition possibilities; ii) a new on-line probe AQUA-MS, which still lacks of data feedback in literature. Consequently, the mass-transfer for H_2S was not studied on the field and barely at lab-scale. Therefore, for future research works, the H_2S mass transfer coefficient was investigated and compared to the O_2 mass transfer coefficient.

Theoretically, the mass transfer only occurs at the liquid side in the laminar diffusion layer, and is related to the diffusivity of the species in water according to equation 1 (Perry and Green, 1985):

$$\boldsymbol{k_{L,i} \propto D_{m,i}^{0.5}} \quad \textbf{(1)}$$

It is thus interesting to use this relation in order to assess the ratio between H_2S and O_2 mass transfer coefficients.

Nevertheless, the exponent 0.5 may not be fully representative of all the hydrodynamic conditions encountered in real sewer networks, and an alternative relation was proposed (equation 2):

$$\frac{K_{L,H_2S}}{K_{L,O_2}} = \left(\frac{D_{m,H_2S}}{D_{m,O_2}} \right)^n \quad \textbf{(2)}$$, where *n* is comprised between 0.5 and 1.

Yongsiri *et al*. (2004a, 2004b) experimentally found a constant ratio $K_{L,H2S}a$ to $K_{L,O2}a$ of 0.86 ± 0.08 at 20°C, independently of the hydraulic conditions in the investigated system.

According to litterature, the gas-liquid oxygen mass transfer is strongly connected to the flow conditions (Table 1). The models gathered in Table 1 were edited on the field. These correlations account for the flow, the slope, the pipe geometry and the turbulence of the system via non dimensional numbers as the Froude and the Reynolds numbers.

Table 1. Empirical models for gas-water oxygen transfer and H_2S emission model

Reaeration Estimation Model		
Authors	**$K_{L,O2}$ a expression**	
Krenkel and Orlob (1962)	$\mathbf{7.235\ (us)^{0.408} d_m^{-0.66}}$	**(3)**
Owens *et al.*(1964)	$\mathbf{0.222\ u^{0.67} d_m^{-1.85}}$	**(4)**
Parkhurst and Pomeroy (1972)	$\mathbf{0.96(1+0.17\ Fr_1^2)(su)^{3/8} d_m^{-1}}$	**(5)**
Taghizadeh-Nasser (1986)	$\mathbf{0.4\ u\ (d_m/R_h)^{0.613}\ d_m^{-1}}$	**(6)**
Jensen (1995)	$\mathbf{0.86\ (1+0.2\ Fr_1^2)(su)^{3/8} d_m^{-1}}$	**(7)**

Since the available models (Table 1) estimate global transfer coefficients and refer to parameters depending on the system geometry (d_m, R_h). It would be useful to dispose of models independent of the geometric dimensions of the system. For this purpose, the main idea was to establish a link between the local mass transfer coefficient and local data, collected at the interface, which is basically not related to the system scale.

This work aimed at measuring the H_2S mass transfer coefficient as a function of the hydraulic characteristics of the flow, with the objective of estimating the H_2S emission in gravity pipes. For safety reasons, the mass transfer coefficient was studied with the oxygen element performed in an experimental gravity pipe (10 m long PVC sewer pipe with internal diameter of 0.2 m) under controlled hydrodynamic conditions. K_L measurements were expressed versus hydraulic as the mean velocity, the Reynolds number or the water height. Meanwhile, experiments for a better

knowledge of the connection between the O_2 transfer and the H_2S transfer were performed in a closed reactor, which can be considered as a small homogeneous volume in a real sewer network system. Furthermore, a new method for the assessment of $K_{L,H2S}$ is proposed.

The numerical modeling tool was used to determine the hydrodynamic parameters at the liquid/gas interface with accuracy, so as to link the mass transfer coefficients to local hydrodynamic parameters.

The real-scale experiments were thus performed with multiple goals: (i) to achieve measurements of O_2 global mass transfer coefficients in a simple real-scale system; (ii) to validate our correlations obtained by mixing numerical modelling and preliminary experimental results in a small homogeneous liquid volume (8 L reactor).

MATERIALS AND METHODS

1. Mass transfer coefficient K_L in a small reactor

a. Experimental approach

Batch reactor experiments were performed in a double wall thermostatic closed vessel in polyvinylchloride of 8 L capacity. The temperature was fixed at 20°C (+/- 0.5°C) and regulated by water circulation in a water jacket. Stirring was ensured by a Rushton turbine made of 4 symmetric blades. For all experiments, the stirring velocity *N* was set between 50 and 140 rpm and controlled by a tachymeter. The calculated dimensionless numbers for stirring were:

- Froude number $\boldsymbol{Fr_1 = \frac{dN^2}{g}}$ **(8)**,
- Reynolds number: $\boldsymbol{Re_1 = \frac{\rho_L N d^2}{\mu_L}}$ **(9),**

The range of values for the stirring velocity corresponds to Reynolds numbers [8,333 – 23,333] and Froude numbers [0.007 – 0.015]. Those mixing conditions were chosen to fall in the turbulent flow regime, which intensifies the mass transfer. The vessel had an interfacial area to volume between 4.73 and 5.11 m^{-1} depending on the surface deformation, which was accounted for by considering the shape of the vortex as a truncated cone. The measurement of the O_2 mass transfer coefficient was based on the conventional re-oxygenation method (American Society of Civil Engineers, 2003; Capela *et al.*, 2004). The experimental procedure consisted in depleting the O_2 content in the liquid phase by adding an adequate amount of sulfite (Na_2SO_3, CAS 7757-83-7) and 1 mg/L of cobalt as a catalyzer ($CoSO_4$, CAS 10026-24-1). O_2 was monitored with an oximeter installed 6 cm under the liquid/gas interface in the liquid bulk (Mettler-Toledo EasySense O_2 21 Oxygen Sensor) and plugged to a computer device and software. The reactor headspace was opened at atmosphere, in order to keep oxygen concentration constant in the gaseous phase. Based on the two film theory, the oxygen concentration during re-oxygenation varied according to equation (10):

$$\boldsymbol{C_{L,O2} = C_{S,O2}(1 - e^{-K_{L,O_2} a\,(t-t_0)})} \qquad \textbf{(10)}$$

The model fitted the experimental results with EXCEL solver by minimizing the sum of the squared differences between experimental and modelled dissolved oxygen concentrations. The adjusted parameters were $K_{L,O2}a$ and $C_{s,O2}$.

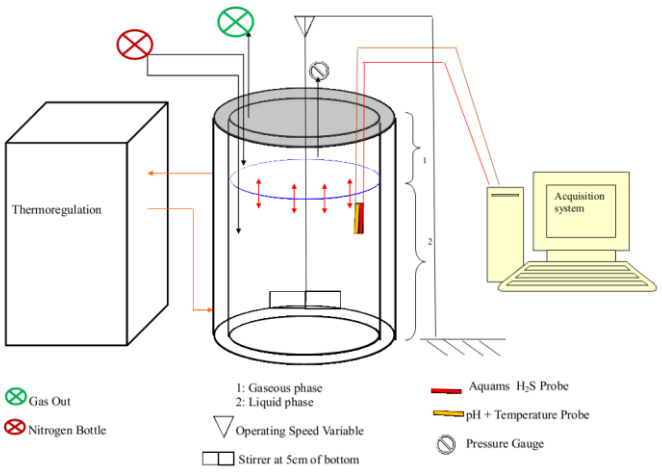

***Figure 1**. Experimental set-up for H_2S mass-transfer coefficient determination.*

For H_2S experiments, the experimental device was isolated from atmosphere and purged with gaseous nitrogen to avoid any chemical reaction between O_2 and H_2S, and H_2S accumulation. The determination of the mass transfer coefficient was made on the basis of a degassing technique. The principle was: i) to create oversaturated conditions by adding a solution of sodium sulfide (Na_2S, $9H_2O$, CAS 1313-84-4) in the liquid phase. The sulfite is rapidly dissolved into HS^- concentration, in equilibrium with dissolved H_2S (around pH 7); ii) to measure the decrease in H_2S concentration with the AQUA-MS probe MS-08, composed of an amperometric sulfide probe combined with pH and temperature measurements; iii) to model the H_2S concentration decrease to determine the mass transfer coefficient.
The variation of concentration was supposed to follow an equation similar to equation (10) according the two film theory: $\boldsymbol{C_{L,H2S} = C_{s,H2S} + (C_{L,0} - C_{s,H2S})e^{-K_{L,H2S}a(t-t_0)}}$,where $C_{L,0}$ is the concentration at $t=t_0$ **(11)**
As oxygen, the model fitted the experimental results with EXCEL solver, by adjusting $K_{L,H2S}a$ and $C_{s,H2S}$. The aim of this experimental part is to establish an empirical correlation between k_L ($m.h^{-1}$) and the mixing velocity (rph) by means of OLS method, in the form of:
$\boldsymbol{k_{L,i} = a_1 + b_1 N^{c_1}}$ **(12)** with a_1, b_1 and c_1 three constants for O_2 and H_2S distinctly.
The $K_{L,H2S}$ / $K_{L,O2}$ ratio was then determined according to the hydrodynamic conditions.

The following part presents the CFD used to describe the velocity fields in the batch reactor and predict the mean velocity at the interface.

b. Numerical approach

CFD approach is usually used to predict the flow field, the velocity components, the turbulent kinetic energy and the turbulent dissipation rate in aerated tanks. In this work, it was used to describe the interface where the mass transfer mainly occurs (Yang and Mao, 2014).

The ICEM CFD™ and FLUENT ™ v.14 software were used to represent the flow pattern and the distribution of the liquid and the gas phases along the flow. A two-fluid model with the Volume of fluid (VOF) and kε-RNG model were chosen to simulate the gas-liquid turbulence. This model was usually employed to simulate multiphase flow (Paul *et al.* 2004): the kε-RNG model is based

on transport equations for the turbulence kinetic energy *k* and its dissipation rate *ε*. Furthermore, the effect of swirl on turbulence was included in the RNG model. In the present study, the kε-RNG model was chosen to strike a balance between the predictive accuracy and the computational economy. The simulation was validated by: i) the y^+ dimensionless number (between 20 and 100), which takes into account the flow velocity and the turbulent quantities at the nodes adjacent to the solid wall; ii) the comparison of the experimental free surface deformation with the numerical description of the interface. A discrepancy inferior to 15% would validate our modeling results.

Many meshes had to be envisaged so as to improve the grid quality and to check that the obtained modeling results were independent of the grid design (Celik *et al*. 2008). The mesh was refined near the impeller blades, the interface and the reactor walls (Figure 2). The mesh quality was specified by an aspect ratio of 22 and an orthogonal quality of 0.69 (Hirsch and Tartinville, 2009). The whole 8 L tank was meshed with 4.1×10^5 hexahedral elements. Finally, the O-grid mesh type chosen to model the reactor is presented in Figure 2 in its bottom section.

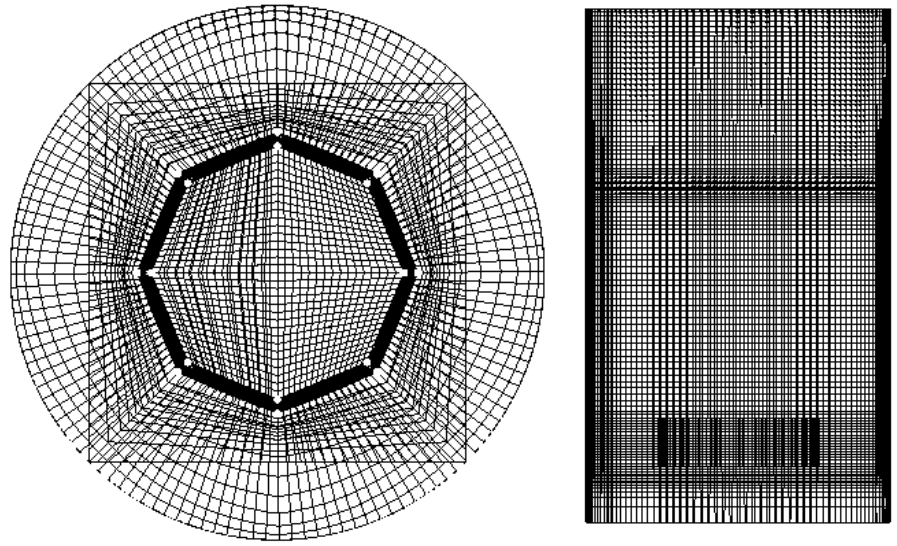

Figure 2*. Computational grid used for the simulations (bottom view at left and lateral view at right)*

The numerical model was simulated in steady flow with a RANS turbulence model. The major purpose was to extract the fluid velocity u_i ($m.h^{-1}$) and the Reynolds number Re_i at the interface:

$$\boldsymbol{Re_i = \frac{\rho_L h\, u_i}{\mu_L}} \quad \textbf{(13)}$$

The hydrodynamic Reynolds number indeed appeared as the most likely to be extrapolated in a real sewerage system. To represent the interface with accuracy, the vortex deformation (height $h=h_{max}-h_{min}$) was selected to be the characteristic dimension, since it is directly governed by the stirring rate and the interfacial conditions. The local velocity used for the Reynolds number calculation was obtained with numerical results.

Then, it was possible to link k_L to the interface parameters so as to improve the equation 12 by including the modeling data so as to obtain equations (14) and (15) as follows:

$$\boldsymbol{k_{L,i} = a_2 + b_2\, u_i^{c_2}} \quad \textbf{(14)}$$

$$\boldsymbol{k_{L,i} = a_3 + b_3\, Re_i^{c3}} \quad \textbf{(15)}$$

with u_i the fluid velocity per surface unit ($m.h^{-1}$) at the interface, Re_i the Reynolds Number (-),a_2, a_3, b_2, b_3, c_2 and c_3 constants determined by a best-fit regression approach (OLS method).

Equations (14) and (15) enable the mass transfer coefficient to be deduced from local parameters describing the interface area. The attempt was made to extrapolate those results to a simplified lab-scale system.

2. Mass transfer coefficient K_L in a real scale gravity pipe pilot

a. Empirical approach

The aim of this part is to measure the mass transfer coefficient in a more realistic system. For safety reasons, the oxygen was chosen to investigate the mass transfer according to parameters easily measurable on the field as the mean velocity, the Reynolds number or the water height. Experiments were carried out in a 10 m long PVC sewer pipe with an internal diameter of 0.2 m (Figure 3). The slope was adjusted between 0 and 2%. Tap water was pumped from a 2 m^3 tank (Mitsubishi E500) and the pumping flow was measured by a flow meter (Rosemount 8732 E).

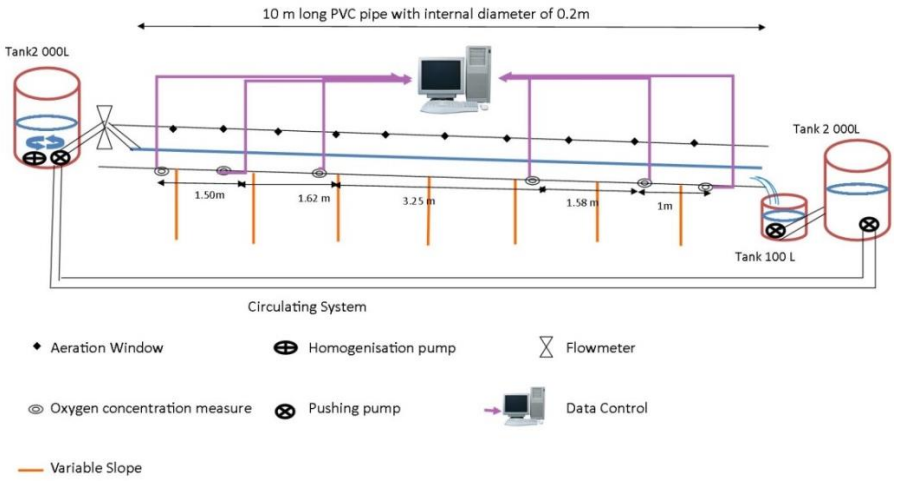

***Figure 3**. Gravity pipe device*

The oxygen concentration was measured continuously by six oxygen probes (Mettler Toledo easySense O_2 21 Oxygen Sensor) located along the pipe length. The controlled and monitored initial parameters were the water flow rate and the initial dissolved oxygen concentration in the tank. Under any flow condition, the height h and the flow width B are sufficient to determine the wetted surface S, the hydraulic diameter d_h and the interfacial area a (Lahav *et al.*,2004). The turbulence is commonly characterized via Reynolds and Froude numbers following these equations:

$$\mathbf{Re_2} = \frac{\rho_L u d_h}{\mu_L} \quad \textbf{(16)} \text{ and } \boldsymbol{Fr_2} = \frac{u}{\sqrt{g d_h}} \quad \textbf{(17).}$$

In this present work, the flow velocities varied between 0.27 and 0.61 m/s, corresponding to Reynolds number values of [4,332 - 46,130] and Froude numbers [0.70 - 0.71].

In steady-state conditions, the mass balance equation reduces to:

$$\frac{dC_{L,i}}{dz} = \frac{-k_L a}{u}\left(C_{L,i} - C_{s,i}\right) \textbf{(18)}$$ where the saturated concentration $C_{s,i}$ is taken from the Winkler table. This equation can then be integrated to calculate the mass transfer coefficient knowing the dissolved concentration $C_{L,i}$.

All experiments, in the reactor and in the pipe, were performed at least in triplicate. Within the replicates, outliers were excluded from the dataset by the statistical method of Thompson (Cimbala J., 2011).

The real-scale system was then described with the CFD simulation tool.

b. Numerical approach

The system geometry was numerically reproduced. The picturing mesh was refined in the water height value (0.55 to 3.55 cm). The mesh quality was specified by an aspect ratio of 19.9 and an orthogonal quality of 0.66. Two meters of the long pipe were meshed with 1.33×10^5 hexahedral elements (Figure 4). The y^+ value and the orthogonal quality validated the mesh design.

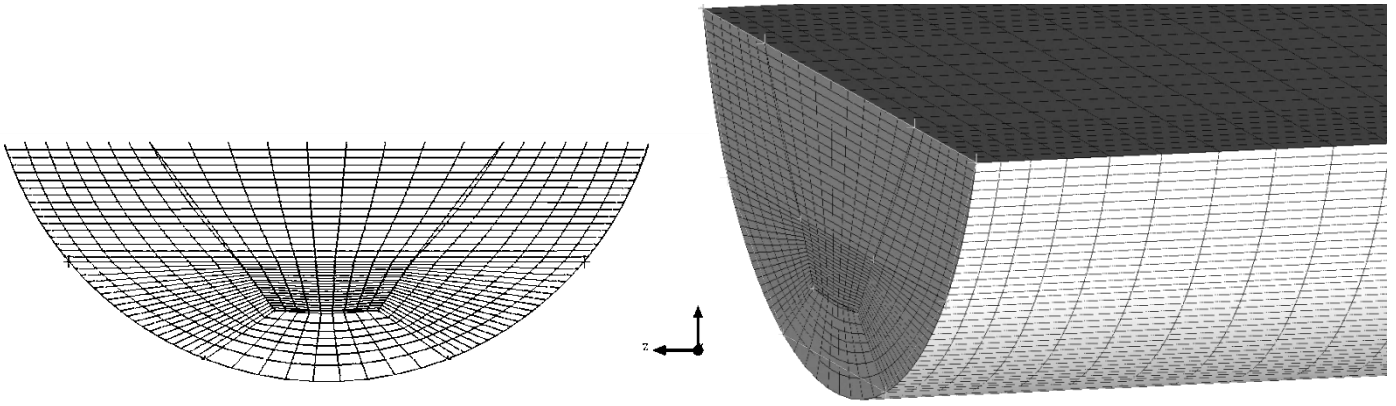

Figure 4*. Computational grid used for the simulations (bottom view at left and lateral view at right) in the pipe*

For numerical calculations, the kε-RNG model was chosen to strike a balance between the predictive accuracy and the computational economy. The velocity and the Reynolds number at the interface were obtained with numerical results, in each cell center. The experimental and the numerical oxygen mass transfer coefficient values were compared to validate the modeling results: a discrepancy inferior to 15% would validate our modeling results. In case the validation criterion would not be fulfilled, the extrapolation would not be confirmed and a new correlation would be edited, on the model of the equations (14) and (15).

Once the numerical description of the flow were obtained, the interface fluid velocity u_i and the Reynolds number Re_i were extracted from the available data.

RESULTS AND DISCUSSION

1. Study of the mass transfer coefficient K_L (O_2 and H_2S) in a small reactor

a. Experimental approach: link between H_2S and O_2 mass transfer coefficient

The H_2S mass transfer and its dependency to the turbulent conditions were studied at the lab-scale, in a small batch reactor. The investigation also aimed at establishing the link between the H_2S and the O_2 mass transfer coefficients.

Figure 5 plots the hydrogen sulfide mass transfer coefficient ($m.h^{-1}$) as a function of the stirring rate (rpm) for all the dataset (35 experiments). $K_{L,H2S}$ exponentially increased with the stirring rate. A similar trend was observed for $K_{L,O2}$ (36 experiments) (results not shown). The exponential evolution of the mass transfer coefficient with the stirring velocity is consistent with the increasing level of turbulence. Indeed, the depth of the liquid film diffusion layer (or the renewal rate of the concentration near the interface) in strongly influenced by the fluid velocity.

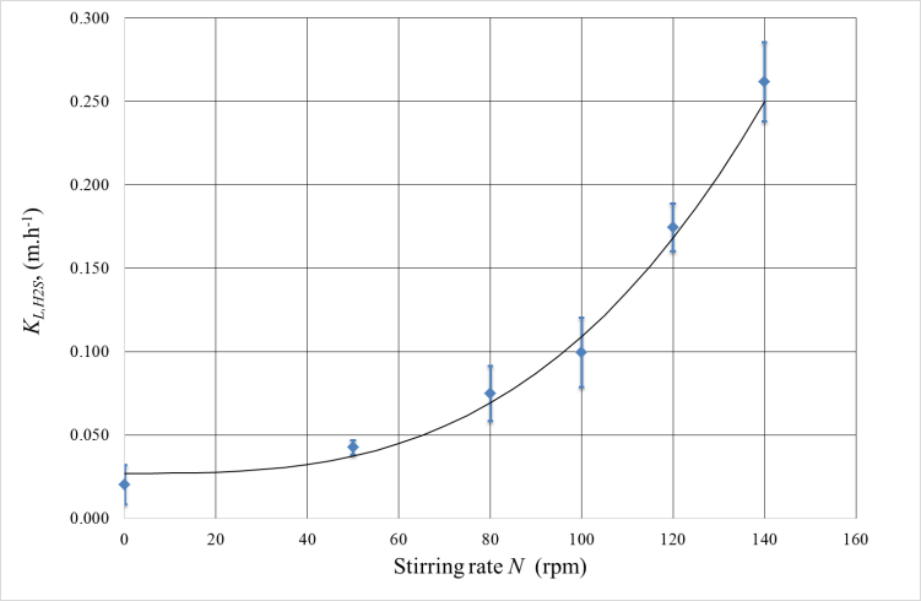

Figure 5. *Influence of the stirring rate mass transfer coefficient of the H_2S ($m.h^{-1}$)*

The following empirical correlations fitted the experimental results:

$$\boldsymbol{K_{L,H_2S} = 0.027 + 0.018\, N^{2.98}} \quad \boldsymbol{(R^2 = 0.98)} \text{ with } N \text{ is in } s^{-1}, K_{L,H2S} \text{ is in } m.h^{-1} \qquad \textbf{(20)}$$

$$\boldsymbol{K_{L,O_2} = 0.015 + 0.025\, N^{3.91}} \quad \boldsymbol{(R^2 = 0.94)} \text{ with } N \text{ is in } s^{-1}, K_{L,O2} \text{ is in } m.h^{-1} \qquad \textbf{(21)}$$

The same tendency was observed by Wu (1995), Vasel (2003) and Parkhurst and Pomeroy (1972). Wu (1995) found in aerated bioreactors an exponential trend for the $K_l a$ as a function of the stirring velocity, where $K_L a$ is proportional to $N^{1.95}$. In rivers and canals, Vasel (2003) found that the mass transfer coefficient is considered proportional to the square root of the velocity. In sewers, the mass transfer coefficient would be proportional to $u^{3/8}$ (Parkhurst and Pomeroy, 1972). Lahav *et al.* (2006) found that the mass transfer coefficient was proportional to the velocity gradient in a sewer pipe.

The following step was to study and compare the mass transfer coefficient between the oxygen and the hydrogen sulfide. Figure 6 plots the experimental mean ratio $K_{L,\,H2S}$ / $K_{L,\,O2}$ as a function of the stirring rate.

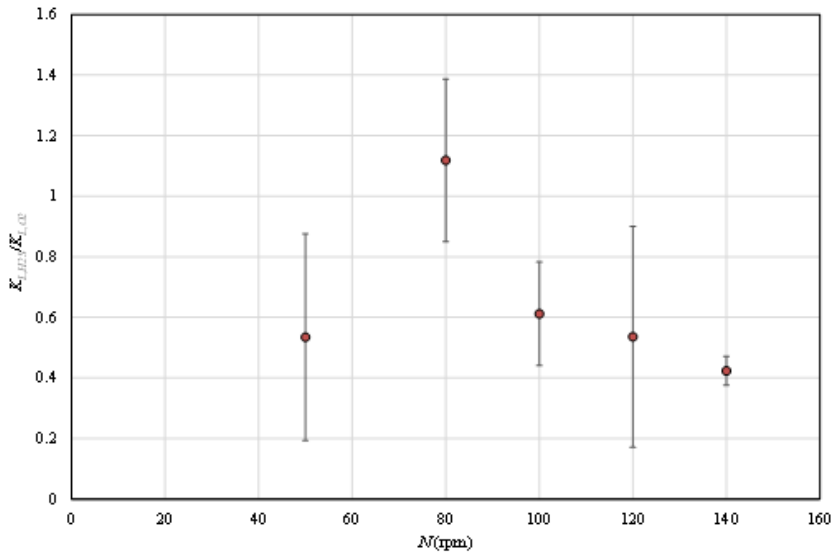

Figure 6. *Influence of the stirring rate on the ration between the hydrogen sulfide mass transfer coefficient (m.h^{-1}) and the oxygen mass transfer coefficient (m.h^{-1})*

The experimental error was symbolized on the figure. The mean ratio was calculated:
$K_{L,\ H2S}$ / $K_{L,\ O2}$ = **0.64 ± 0.24 (22)**. Given the uncertainty, this value falls in the range of the diffusivity ratio (D_{H2S}/D_{O2} = 0.86). The rate of the H_2S transfer was generally lower than the reaeration process and exhibits a similar behavior. In 1974, USEPA suggested that $K_{L,H2S}a$ / $K_{L,O2}a$ ratio was 0.72, which is consistent with our conclusions.

b. Numerical approch

The modeling results of the flow characteristics in the stirred reactor highlighted no dead zone, and the velocity fields evidenced a homogeneous mixing in the liquid volume. Therefore, the system description is consistent with the basic assumptions needed to apply the two film theory. For the lowest stirring velocity (50 rpm), the local velocities ranged between 0.009 and 0.118 (mean value of 0.103). For the highest stirring velocity (140 rpm), the local velocities were modeled in the range of values [0.009 - 0.418] (mean value of 0.273 m.s^{-1}).

The mean velocity modeled in the liquid film was found proportional to the stirring rate with a good accuracy:

$\mathbf{u_i = 0.1175\ N}$ (r^2 = 0.98), with u_i in m.h^{-1}, and N in rph **(23)**

This correlation is fully dependent on the experimental set-up, and therefore the extrapolation to other systems is impossible. Nevertheless, it was of interest from a methodology viewpoint. A correlation made from the numerical modeling results may be similarly written involving the interface Reynolds number.

Those results were then added to the experimental measurements of k_L through the interface. For instance, merging equation 23 with the equation 21 enables the oxygen transfer coefficient to be expressed as a function of the flow conditions at the interface:

$\boldsymbol{K_{L,O2} = 0.015 + 1.35 \times 10^{-12}\ u_i^{3.91}}$. with u_i in m.h^{-1} **(24)**

With the OLS method, Equation 25 was as well edited:

$\boldsymbol{K_{L,O2} = 0.0677 + 2.098 \times 10^{-9} Re_i^{2.147}}$ **(r^2= 0.99)** **(25)**

Those results make the estimation of the oxygen transfer mass coefficients possible in systems of different geometries, provided that the hydrodynamic conditions are in the same range of

values and provided that local turbulent conditions are accessible with numerical modeling tools as CFD. The following part presents the study of the mass transfer in a real scale system.

2. Study of K_La in gravity pipe with oxygen

a. Experimental approach

The hydrodynamic character in the real scale device were determined as follows: i) subcritical flow, i.e. a flow controlled from a downstream point and transmitted in the upstream (Fr_2<1); ii) turbulent flow (Re_2> 4,000), iii) velocities lower than 0.45 m.s^{-1} that engender axial dispersion flow, and higher than 0.45 m.s^{-1} (30 % of tested velocities) that reflect plug flow.

Figure 7 plots the oxygen mass transfer coefficient (m.h^{-1}) as a function of the mean velocity (m.s^{-1}). $K_{L,O2}$ exponentially increased with the mean velocity. The exponential evolution of the mass transfer coefficient with the velocity is consistent with the increasing level of turbulence, which is the same tendency observed during the experiments in the small reactor.

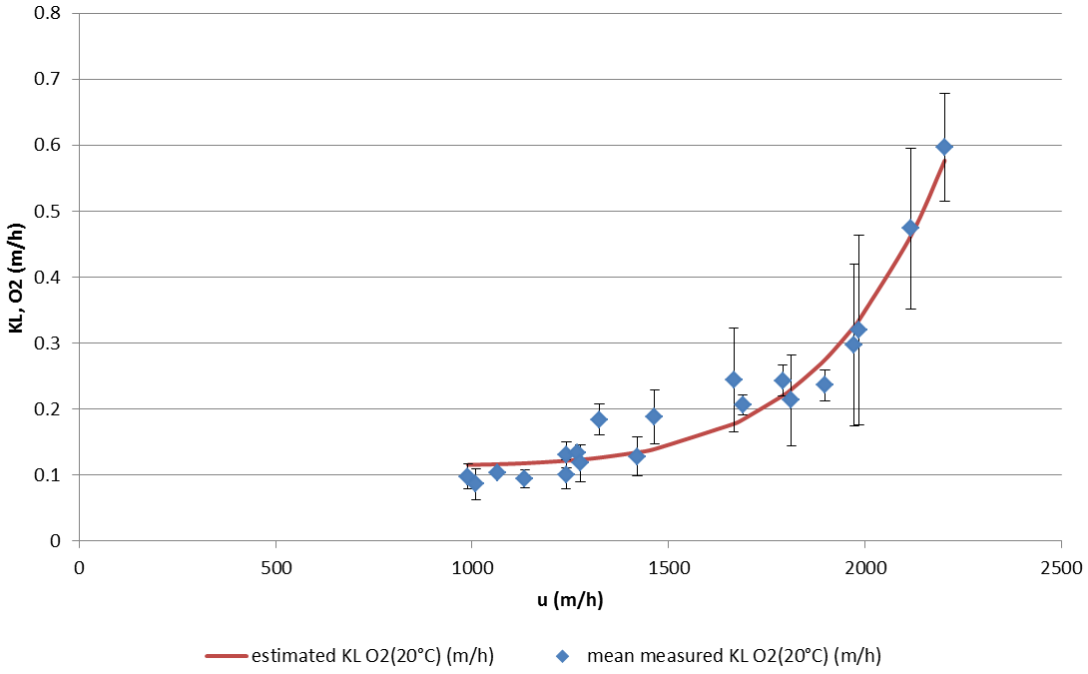

Figure 7. *Flow velocity (m.h^{-1}) effect on the oxygen transfer coefficient (m.h^{-1})*

Correlations can be edited, with the mean velocity for instance, as the equation 26:

$$\boldsymbol{K_{L,O2} = 0.117 + 9.19 \times 10^{-25}\, u^{7.09}} \quad \boldsymbol{(R^2 = 0.97)} \qquad \textbf{(26)}$$

The advantage of this kind of correlation is o depend on a single parameter, and to be easily usable on the field. The $K_{L,O2}$ value estimates with equation (26) were in agreement with Parkhurst and Pomeroy (1972), Krenkel and Orlob (1962), Taghizadeh and Nasser (1986) and Jensen (1995), with observed mean differences of 70%, 51%, 23% and 58 % respectively.

Equation 26 can be reused by applying a coefficient of 0.64 in order to estimate the H_2S transfer coefficient and H_2S emission conditions can be deduced via the equation 22 in the same hydraulic conditions.

b. Numerical approach

In the real-scale device, the numerical approach was used for several purposes: i) study the dependency of k_L on hydraulic conditions in a real system; ii) extract the hydraulic conditions at the interface, similarly to the work achieved in the reactor system; iii) predict the k_L results with the equations (24) and (25); iv) draw conclusions about the possible extrapolation of those numerical and empirical results. Conversely, the obtained correlations would be refined.

As in the small reactor, once the simulation grid was designed and approved, and the accuracy of the modeling results verified, the flow was described in the pipe. The overall flow hydraulic patterns were examined. The hydraulic conditions in the liquid-gas boundary layer, the local velocity and the Reynolds number, were extracted from the modeling results. With the correlations previously established, the expected O_2 mass transfer coefficients were calculated and compared to the experimentally measured mass transfer coefficients.

CONCLUSION

To highlight the mechanisms and the dynamics of hydrogen sulfide emission in real conditions, some approaches were adopted. In litterature, the gas-liquid oxygen mass transfer is strongly connected to the flow conditions. The purpose of this research work was to collect more data to establish models independent of the system geometry. For this goal, several scales were investigated: at lab-scale, a batch reactor device, similar to a homogeneous liquid volume was experimented and, at real-scale, a gravity pipe device with continuous water flow was set up.
In the reactor, the behavior of the H_2S mass transfer was studied versus the turbulent conditions (Reynolds range values [0-23,333] and Froude range values [0-0.97]) and then compared to the O_2 mass transfer coefficient. $K_{L,H2S}$ as well as $K_{L,O2}$ were shown to increase exponentially with the turbulence intensity, which is consistent with an increasing level of turbulence. The mean ratio $K_{L,H2S}/K_{L,O2} = 0.64 \pm 0.24$ was obtained. Correlations were edited to link the mass transfer coefficient to hydraulic parameters as the Reynolds number or the mean velocity in the liquid phase. With the CFD modeling tool, those correlations were refined by expressing local interface conditions, so as to make the equations independent of the averaged hydraulic parameters of the system. These results were then applied to real size system. The discrepancy between the measured and the predicted $K_{L,O2}$ mass transfer coefficients were discussed. These equations are expected to be valid on the field and to simplify the modeling and the prediction of the phenomena linked to O_2 and H_2S liquid-gas mass transfer in sewer networks.

REFERENCES

American Society of Civil Engineers. 2003 ASCE Standard measurement of oxygen transfer in clean water, New York.

Capela S., Gillot, S., Héduit A. 2004 Comparison of oxygen transfer measurement methods under process conditions. *Water Environment Research,* **76**(2), 183-188.

Carrera L., Springer F., Lipeme-Kouyi G., Buffiere P. 2015 A review of sulfide emissions in sewer networks: overall approach and systemic modelling. *Water Science & Technology,* **73**(6). DOI: 10.2166/wst.2015.622

Celik I.B., Ghia U., Roache P.J., Freitas C.J., Coleman H., Raad P.E. 2008. Procedure for Estimation and Reporting of Uncertainty Due to Discretization in CFD Applications. *J. Fluids Eng,* 130(7), *078001*-4.

Cimbala J. 2011 Outliers. Presentation, Pennsylvania State University. (http://www.mne.psu.edu/me345/Lectures/Outliers.pdf)

Hirsch C. and Tartinville B. 2009 Reynolds-Average Navier-Stokes modelling for industrial applications and some challenging issues. *International Journal of Computational Fluid Dynamics*, 23(4), 295-303.

Jensen N.A. 1995 Empirical modeling of air-to-water oxygen transfer in gravity sewers. *Water Environment Research,* **67**(6), 979–991.

Krenkel P. and Orlob G.T. 1962 Turbulent diffusion and the reaeration coefficient. *Journal of the Sanitary Engineering Division, ASCE.* **88**(2), 53-83.

Lahav O., Lu Y., Shavit U. and Loewenthal R. 2004 Modeling hydrogen sulphide emission rates in gravity sewage collection systems. *Journal of Environmental Engineering,* **130**(11), 1382–1389.

Lahav O., Sagiv A. and Friedler E. 2006 A different approach for predicting $H_2S_{(g)}$ emission rates in gravity sewers. *Water Research,* 40(2), 259–266.

Owens M., Edwards E.W. and Gibbs J.W. 1964 Some reaeration studies in streams. *International Journal of Air Pelution,* **8**, 469-486.

Parkhurst J.D. and Pomeroy R.D. 1972 Oxygen absorption in streams. *Journal of the Sanitary Engineering Division, ASCE*. 98(SA1), 101–124.

Paul E, Atiemo-Obeng A., Kresta S. 2004 Handbook of industrial mixing: Science and Practice. New York: John Wiley.

Perry R.H., Green D. 1985 Perry's Chemical Engineers Handbook, 6th edition, McGraw Hill.

Taghizadeh-Nasser M. 1986 Gas-liquid mass transfer in sewers (in Swedish); Materieöverföring gas- vätska I avloppsledningar, Chalmers Teckniska Högskola, Göteborg, Publikation, 3:86 (Licentiatuppsats).

US.Environmental Protection Agency. 1974 Process Design Manual for Sulfide Control in Sanitary Sewerage Systems. *US Environmental Protection Agency Technology Transfer Office, Washington, DC EPA,* 625/1-74-005.

Vasel J-L. 2003 Aération naturelle dans les procédés d'épuration à biomasse fixée et les écosystèmes aquatiques, *in* M. Roustan, *« Transfert gaz-liquide dans les procédés de traitement des eaux et des effluents gazeux »*, Lavoisier Tec&Doc, Chapter 10, 445-488

Wu H. 1995 An issue on applications of a disk turbine for gaz-liquid mass transfer. *Chemical Engineering Science*, 50(17), 2801-2811.

Yang C. and Mao Z.S. 2014 Numerical Simulation of multiphase reactors with continuous liquid phase. *Chemical Industry Press,* 1rd edition Elsevier, Oxford, UK.

Yongsiri C., Vollertsen J. and Hvitved-Jacobsen T. 2004a Effect of temperature on air–water transfer of hydrogen sulfide. *Journal of Environmental Engineering*, 130(1), 104–109.

Yongsiri C., Vollertsen J. and Hvitved-Jacobsen T. 2004b Hydrogen sulfide emission in sewer networks: a two-phase modelling approach to the sulfur cycle. *Water Science and Technology*, 50(4), 161–168.